Int. J. Heat Mass Transfer. Vol. 19, pp. 1299–1307. Pergamon Press 1976. Printed in Great Britain

AN ANALYSIS OF THE EFFECT OF SURFACE THERMAL CONDUCTIVITY ON THE RATE OF HEAT TRANSFER IN DROPWISE CONDENSATION

R. J. HANNEMANN
Bell Telephone Laboratories, Whippany, NJ 07981, U.S.A.

and

B. B. MIKIC
Massachusetts Institute of Technology, Cambridge, MA 02139, U.S.A.

(*Received* 22 *September* 1975 *and in revised form* 19 *February* 1976)

Abstract—An analysis of the effect of the condenser material thermal properties on the dropwise condensation heat-transfer coefficient is reported here. The synthesis of single-droplet constriction resistance solutions with the known droplet distribution leads to a simple correlation for the effect. The correlation agrees well with the bulk of existing experimental data for water; other fluids may be treated via the analytical path developed.

NOMENCLATURE

A, surface area;
C, coefficient in constriction conductance correlation;
h, heat-transfer coefficient;
h_a, "active" area conductance;
h_c, constriction conductance;
h_c^*, constriction conductance in adiabatic cylinder problem;
h_d, average heat-transfer coefficient under a condensate droplet;
$\bar{h}_d$, dropwise condensation surface average conductance in the absence of constriction effects;
h_i, "inactive" area conductance;
h_p, average heat-transfer coefficient over area covered by primary drops;
h_s, surface average heat-transfer coefficient, $\frac{1}{A}\int_A h_{\text{local}}\,dA$;
k, thermal conductivity of condenser material;
k_l, thermal conductivity of condensate;
L, cylinder height in adiabatic cylinder problem;
$N(r_1, r_2)$, total number of drops per unit area with radii between r_1 and r_2;
$N^*(r)$, droplet distribution function;
q, heat flux;
R, adiabatic cylinder radius;
r, droplet radius, radial coordinate;
r_d, droplet radius;
r_0, smallest drop radius in macroscopic drop distribution;
$\hat{r}$, radius of departing drops;
T, temperature;
T_{local}, local surface temperature;
T_0, constant base temperature in adiabatic cylinder problem;
T_s, average condensing surface temperature;
T_{sat}, saturation temperature;
T_v, vapor temperature;
z, axial coordinate.

Greek symbols

$\alpha(r)$, fraction of condenser surface area covered by drops with radii larger than r;
γ, ratio of "inactive" area conductance to "active" area conductance;
ζ, nondimensional adiabatic cylinder length coordinate;
η, dimensionless drop size;
θ, dimensionless temperature in adiabatic cylinder problem;
ρ, nondimensional radial coordinate.

Dimensionless groups

Bi, condensation Biot number $\left(\frac{h\hat{r}}{k}\right)$;
Bi_a, "active" area Biot number $\left(\frac{h_a R}{k}\right)$;
Bi_c, constriction Biot number $\left(\frac{h_c \hat{r}}{k}\right)$;
Bi_c^*, single-droplet constriction Biot number $\left(\frac{h_c^* R}{k}\right)$;
Bi_d, condensation Biot number in the absence of constriction effects $\left(\frac{\bar{h}_d \hat{r}}{k}\right)$;
Bi_d^*, single-droplet Biot number $\left(\frac{h_d R}{k}\right)$;

Bi_s, surface average Biot number in adiabatic cylinder problem $\left(\frac{h_s R}{k}\right)$;

Nu_d, pre-constriction condensation Nusselt number $\left(\frac{\bar{h}_d \hat{r}}{k_l}\right)$.

1. INTRODUCTION

DROPWISE condensation is a complex simultaneous heat- and mass-transfer process dependent on the surface at which the condensation occurs as well as the fluid of interest and ambient conditions. Technological interest in the phenomena is due to the enhanced heat transfer possible: conductances 30–40 times larger than those in filmwise condensation have been observed.

Much progress has been made in understanding the underlying physical phenomena of dropwise condensation since it was first observed by Schmidt *et al.* [1] in 1930. Some early theoretical work (e.g. the model due to Jakob [2]) was based on the premise that droplets form from the fracturing of a thin layer of condensate; gradually, it was recognized that the mechanism of droplet formation is, in fact, due to nucleation.

Recent theoretical work has been concentrated on integrating single-drop heat-transfer results over the entire droplet distribution [3, 4] and digital computer simulation of the dropwise condensation process [5–8].

These theoretical treatments do not consider the effects of condensing surface thermal properties. Because there is a distribution of drops of widely varying size present on the condensing surface during dropwise condensation, portions of the surface (bare areas and areas under the large drops) are effectively insulated, while adjacent areas have extremely high heat-transfer rates. This nonuniformity of surface heat flux leads to a thermal resistance in addition to the average droplet resistance, caused by the constriction of the heat flow lines near the condensing surface. The possible importance of this thermal constriction resistance was recognized and studied by Mikic [9].

The work to be reported here consists of an analysis and correlation of the thermal constriction resistance in dropwise condensation and a subsequent comparison of this theory to existing experimental evidence.

2. THEORETICAL AND EXPERIMENTAL BACKGROUND

If a large enough area is taken as the region of interest, the size distribution of droplets during dropwise condensation is found to be statistically stationary; that is, the number of drops in a given size range per unit condensing surface area remains constant in time. Once the distribution of drop sizes is known, models for calculating the average heat transfer for an entire surface may be constructed based on the heat-transfer resistances in single drop heat flow.

The drop distribution is most conveniently presented in terms of the distribution function $N^*(r)$ defined by

$$N^*(r) = \lim_{\Delta r \to 0} \frac{\Delta N(r)}{\Delta r}, \qquad (1)$$

where ΔN is the total number of drops per unit area with radii in the interval $(r-(\Delta r/2), r+(\Delta r/2))$. Much useful information can be extracted from the droplet distribution function, such as the number of drops per unit area in a given finite radius interval, $N(r_1, r_2)$, and the fraction of surface area covered by drops larger than a given radius, $\alpha(r)$.

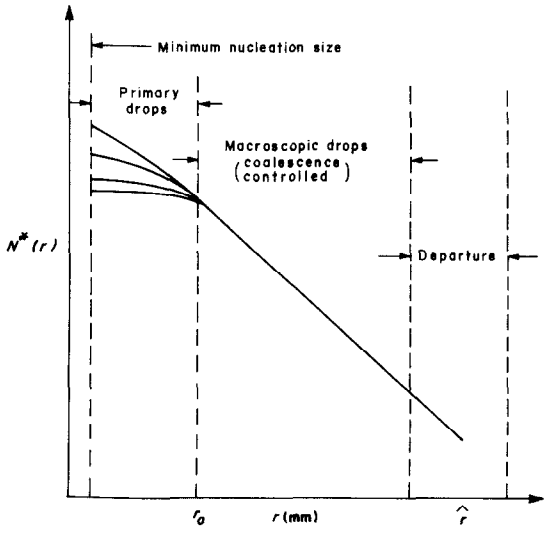

FIG. 1. The droplet distribution function.

An idealized drop distribution is depicted in Fig. 1, illustrating several important subdivisions. Primary drops are microscopic drops which grow by direct condensation with few coalescences. The number of primary drops is a function of the total available area (i.e. area not covered by larger drops) and the number of nucleation sites per unit area. A large portion of the total heat flow is through drops in this relatively narrow band of radii. Experimental evaluation of the primary drop distribution is extremely difficult due to the rapid growth and small size of these droplets.

The drop distribution in the range of radii in which the drop growth is coalescence-controlled appears to be universal [10], that is, independent of heat transfer and surface parameters (at least for water on moderately sized condensers, the only situation for which detailed drop distributions have been measured). Agreement between various measured drop distributions in the coalescence-controlled region is good, as can be seen from Fig. 2. Although much of the heat transfer is carried on by the microscopic drops, the macroscopic drops affect the area available for primary drops and the thermal constriction resistance, so that this region is important for the modeling of the overall surface heat-transfer coefficient.

The departure size $\hat{r}$, i.e. the average radius at which drops begin to slide from the surface, depends on the fluid-surface combination, surface roughness, condenser orientation, gravitational force, and vapor velocity. Although departure size does not have a marked effect on the form of the macroscopic drop distribution, it is a controlling factor for the primary drop distribution, since any area covered by departure

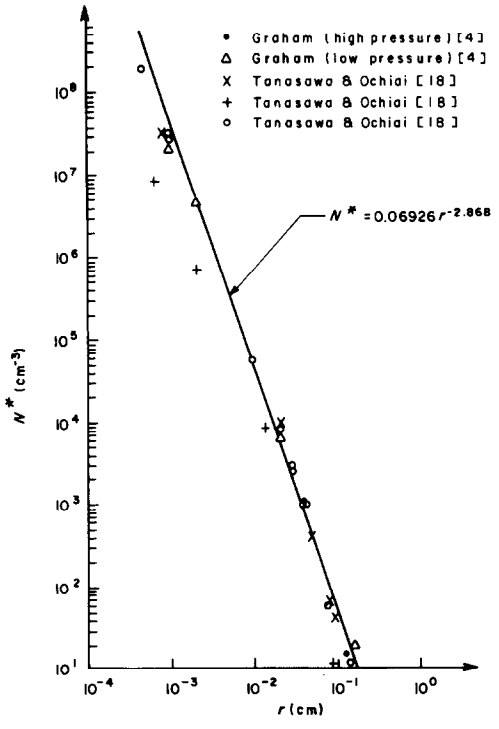

FIG. 2. Experimental droplet distribution data.

and near departure sized drops is unavailable for the formation of primary drops.

The constriction resistance theory which has been developed takes the overall surface conductance in the absence of constriction resistance (i.e. the surface heat-transfer coefficient for a condenser with infinite lateral conductivity) into account as a parameter. This heat-transfer coefficient, $\bar{h}_d$, can be readily estimated from experimental measurements on high conductivity (copper) surfaces.

The surface conductance is defined in the usual way, that is,

$$h = \frac{q}{T_v - T_s}, \tag{2}$$

where q is the average heat flux, T_v is the vapor temperature, and

$$T_s = \frac{1}{A}\int_A T_{\text{local}}\,\mathrm{d}A. \tag{3}$$

T_{local} is the spacewise (and timewise) varying local surface temperature, and A is the surface area under consideration. In the absence of surface thermal property effects, it is also true that

$$h = \frac{1}{A}\int_A \frac{q}{T_v - T_{\text{local}}}\,\mathrm{d}A, \tag{4}$$

but equation (4) is not valid if the surface temperature or heat flux varies. In such a case, there is an additional thermal resistance in series with the surface average conductance through the droplets, which statement can be written mathematically as

$$\frac{1}{h} = \frac{1}{\bar{h}_d} + \frac{1}{h_c}. \tag{5}$$

Here h is defined by equation (2), $\bar{h}_d$ is the surface average conductance through the drops, and h_c is the thermal constriction conductance.

Experimental evidence has been gathered which suggests that the constriction conductance h_c is finite. At least four investigations have produced relevant data on the surface thermal property effect on the heat-transfer coefficient in dropwise condensation [11–14]. The first three of these studies show a substantial constriction resistance effect, while the fourth does not; a detailed discussion of the data is contained elsewhere [16]. The theory developed in this paper will be compared to the existing data in due course.

3. THE THERMAL CONSTRICTION RESISTANCE ATTENDANT TO A SINGLE LARGE DROP

The approach taken in developing a model for the constriction resistance was to analyze first the constriction resistance arising from a single macroscopic drop surrounded by numerous microscopic or "active" drops. To this end, a necessary preliminary step is the determination of the conductance through a droplet due to conduction and other effects.

The various resistances to heat flow through a drop have been thoroughly discussed elsewhere [15, 16]. For "macroscopic" drops (say, drops with radii larger than 0.005 cm) in "gas free" systems, the thermal resistance due to pure conduction predominates. A simple but accurate approximation for a hemispherical droplet [9] is

$$h_d = \frac{4k_l}{r_d}, \tag{6}$$

wherein h_d is the average conductance seen by the condensing surface under a droplet, r_d is the droplet radius, and k_l is the condensate thermal conductivity.

The droplet conductance (6) is an average conductance over the drop base area. Since the conduction path through the liquid is shorter near the edge of a drop, the conductance there is higher. With this in mind, the variation of the heat transfer coefficient in the vicinity of a single large drop surrounded by numerous smaller drops is sketched in Fig. 3.

The area over which the very high edge heat-transfer coefficients act is quite small, however. The size of the large drop is an order of magnitude larger than the surrounding smaller drops, and spatial variations in the heat-transfer coefficients over the base area of the drop and outside the large drop also occur on different scales.

It is assumed that the heat-transfer coefficient variation may be approximated by the step function shown in Fig. 3. The drop conductance h_d is simply the average heat-transfer coefficient over the large drop base area, while the "active" area heat-transfer coefficient h_a is the area average heat-transfer coefficient for the area outside the large drop, and may include a constriction conductance term for thermal constriction on a scale smaller than that associated with the large drop.

The fundamental heat-conduction problem defined by the configuration of Fig. 3 (with radial heat flow zero at some "adiabatic cylinder" radius R) was solved

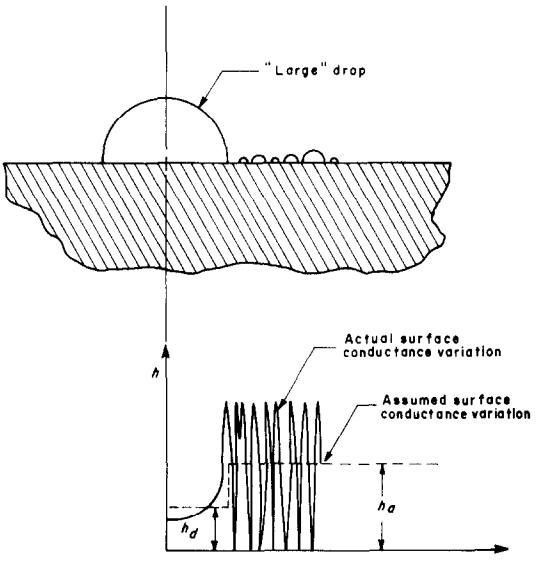

FIG. 3. Surface conductance variation in dropwise condensation.

in nondimensional form for a large range of parameters for use in the overall constriction model of Section 4 (see the Appendix). Typical results are shown in Fig. 4.

The ordinate of this plot represents the ratio of the constriction resistance to the average surface resistance, while the abscissa is the ratio of the large-drop radius to the adiabatic cylinder radius considered. The parameters used are defined in the Figure and the Appendix.

From examination of this plot, it can be seen that the results are well behaved. For a given conductance ratio γ and droplet Biot number Bi_d^*, the constriction resistance first increases, then decreases with the drop size η, as would be expected. At $\eta = 0$ and $\eta = 1$, the constriction resistance must be zero, since then no step in surface conductance is present. As γ increases, that is, as the step function surface boundary condition becomes less pronounced, the constriction resistance decreases, as it should. Finally, as Bi_d^* increases, the constriction resistance decreases. This is appropriate, for as Bi_d^* increases with constant γ and η, the surface conductance nonuniformity becomes less important. (Increased Bi_d^* arises, for example, from an increase in R; this increase in scale implies a decrease in the relative importance of the constriction resistance.)

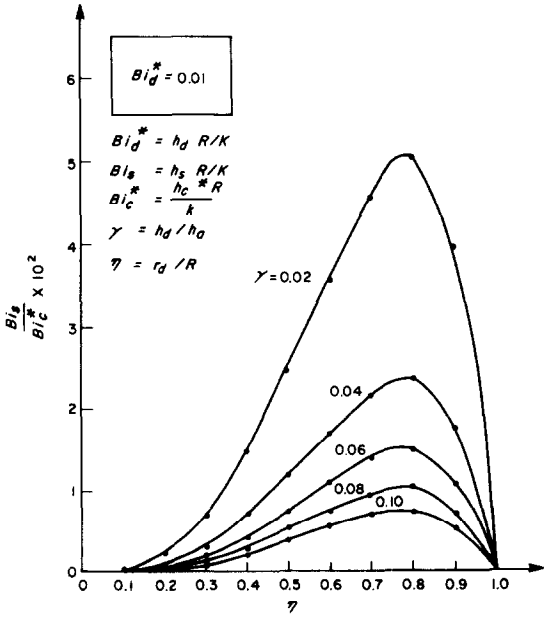

FIG. 4. Typical single-droplet constriction resistance results.

4. THE OVERALL CONSTRICTION RESISTANCE MODEL

In calculating the overall thermal constriction resistance it is assumed that:

1. The droplet distribution is statistically stationary, with the macroscopic drop distribution being universal.
2. The droplet distribution is taken to be spatially random. Each drop is considered to be centered on a disc of surface area with which the droplet is associated. (Consideration of eccentricity in thermal contact resistance calculations leads to the conclusion that for a maximum offset, the thermal constriction resistance increases by less than a factor of $\sqrt{2}$; this has been verified by experiment [15]. Since in the present case the eccentricity should be much less than the maximum, the assumption of a random droplet distribution (no eccentricity) is justified.)
3. The time response of the surface to changing heat-transfer coefficients is sufficiently rapid and thermal storage effects sufficiently small that the steady-state conduction equation in the condenser material is valid [16]. The time for coalescence of macroscopic drops is assumed to be much smaller than the time between coalescences, so that steady-state conduction can be assumed for calculating the droplet heat transfer resistance.
4. The constriction resistance due to precoalescence drops can be neglected. (This can be shown *à posteriori* from the model described here.)

In order to describe the model, it is necessary to introduce the idea of distinct drop classes. The nomenclature is introduced in Fig. 5. The range of radii for which the drop distribution N^* is heat flux and surface dependent is called the primary drop class. (The lower limit on radius is taken to be zero, so that bare area is included as area covered by drops of the primary drop class; the smallest coalescence-controlled drop has a radius r_0. For steam condensation, the choice $r_0 = 5$ micrometers is appropriate from the standpoint of the constriction resistance as well as the droplet distribution.)

Each drop class may be assigned properties which are representative of the drops of that class. The total number of drops in the ith drop class is given by

$$N_i = N(r_{i-1}, r_i) = \int_{r_{i-1}}^{r_i} N^*(r)\,dr, \qquad (7)$$

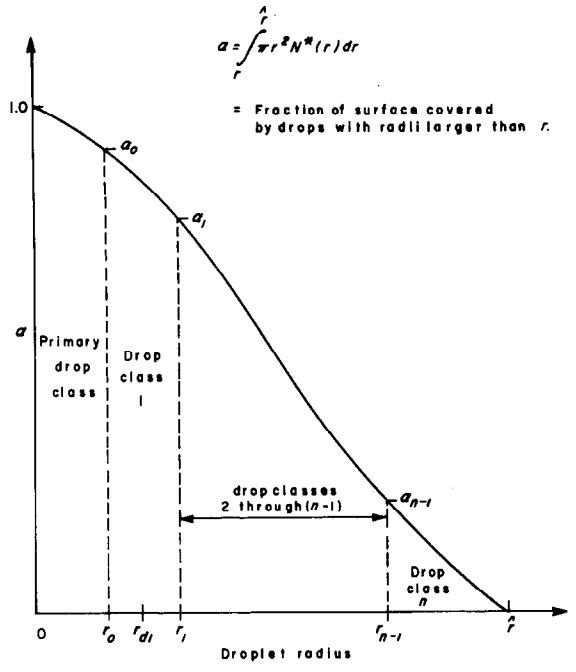

FIG. 5. Drop class nomenclature.

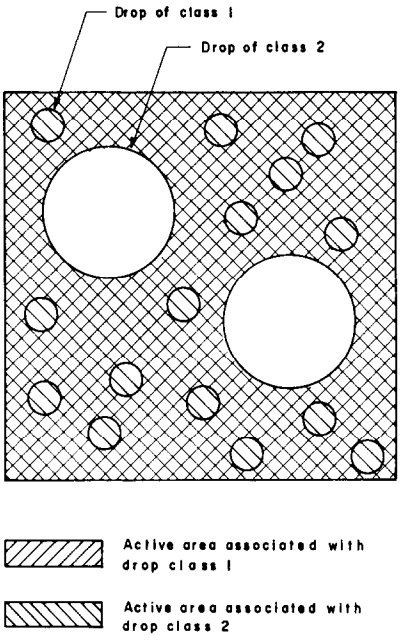

FIG. 6. Surface area assignation to drop classes.

while the fraction of area covered by these drops is

$$\Delta\alpha_i = \alpha_{i-1} - \alpha_i = \int_{r_{i-1}}^{r_i} \pi r^2 N^*(r)\,dr. \tag{8}$$

A typical drop size can then be defined through the equation

$$\pi r_{di}^2 N_i = \Delta\alpha_i. \tag{9}$$

Finally, the average droplet heat-transfer coefficient in the absence of constriction for each drop class can be calculated:

$$h_{di} = \frac{1}{\Delta\alpha_i} \int_{r_{i-1}}^{r_i} h_d(r)\left(-\frac{d\alpha}{dr}\right) dr. \tag{10}$$

Drops in each drop class are presumed to be surrounded and influenced by drops smaller than themselves. Thus, drops of class 1 are taken to be completely surrounded by primary drops, drops of class 2 are taken to be located within areas otherwise populated by drops of the primary class and class 1, and so on. Surrounding area is referred to as active area, as opposed to the relatively inactive area directly under a drop. The area assignation concept is illustrated for a two-drop-class system in Fig. 6.

If the drop distribution is spatially random, as it is assumed to be, "adiabatic cylinder" subproblems for the typical drops of each drop class can be defined and solved sequentially in order to arrive at the constriction resistance for the entire surface.

Consider, for example, the two macroscopic drop class system of Fig. 6. As assumed at the outset, the microscopic or primary drops do not have a significant constriction resistance associated with them. Thus, if the surface heat-transfer coefficient $\bar{h}_d$ for a material of infinite lateral conductivity is known or assumed, the average heat-transfer coefficient over the cross-hatched area, h_p, may be calculated from the equation

$$\bar{h}_d = (1 - \Delta\alpha_1 - \Delta\alpha_2)h_p + \Delta\alpha_1 h_{d1} + \Delta\alpha_2 h_{d2}, \tag{11}$$

where the $\Delta\alpha$'s are known from the droplet distribution and equation (10) is used for h_{d1} and h_{d2}.

The crosshatched area can be apportioned among the droplets of class 1 since their number per unit area is known, as is the area covered by primary drops. This defines an adiabatic cylinder radius for class 1:

$$R_1 = \left[\frac{1 - \Delta\alpha_2}{\pi N_1}\right]^{\frac{1}{2}}. \tag{12}$$

For a particular surface conductivity, all the dimensionless parameters needed to obtain the constriction resistance associated with droplets of class 1 can be determined. The constriction conductance h_{c1} is then obtained from single-droplet results, with the "true" average conductance over the area covered by primary drops and drops of class 1 being calculable from the equation

$$\frac{1}{h_1} = \frac{1}{h_{s1}} + \frac{1}{h_{c1}}. \tag{13}$$

(The conductance h_{s1} is the area weighted average of h_{d1} and h_p here.)

It should be apparent that the constriction resistance associated with drops of class 2 can now be calculated; the active area conductance to be used is the true average conductance obtained from the previous step, h_1. For a two-drop-class model, the conductance h_2 calculated from

$$\frac{1}{h_2} = \frac{1}{h_{s2}} + \frac{1}{h_{c2}} \tag{14}$$

is then the overall dropwise condensation conductance h for a condenser material of conductivity k with a heat-

transfer coefficient in the absence of constriction equal to $\bar{h}_d$. The overall constriction conductance h_c is determined via the equation

$$\frac{1}{h} = \frac{1}{\bar{h}_d} + \frac{1}{h_c}. \tag{15}$$

In a manner analogous to that described above for a two-class model, many-class models were treated for varying conductivity k, asymptotic conductance $\bar{h}_d$, and departing droplet size $\hat{r}$. As the number of classes was increased, the calculated constriction effects approached a limiting value. These limiting values were used as an estimate of the true constriction effect in the construction of the constriction resistance correlation described below.

5. CORRELATION OF RESULTS AND COMPARISON TO DATA

The number of variables which affect dropwise condensation heat transfer is quite large. Surface microproperties, system pressure, surface orientation, promoter, condenser thermal conductivity, noncondensable gas concentration, contact angle, and departure radius all play important roles. Assuming that there is a universal distribution for large drops, however, the constriction resistance component of the total surface resistance can be correlated in a relatively simple fashion.

It was found possible to represent the results in the form

$$Bi_c = C \cdot \left(\frac{k}{k_l}\right)^{-m}, \tag{16}$$

where

$$Bi_c = \frac{h_c \hat{r}}{k} \tag{17}$$

is the constriction Biot number and k/k_l is the ratio of the material and condensate thermal conductivities. In the relationship (16), C is found to depend on the Nusselt number $\bar{h}_d \hat{r}/k_l$ and the ratio of characteristic lengths $r_0/\hat{r}$; the exponent m depends only on the Nusselt number.

In many problems, the thermal constriction conductance is directly proportional to the material conductivity, i.e. $m = 0$. This relationship holds for applied heat flux or temperature step function boundary conditions, appropriate for thermal contact resistance problems, for example. The applied heat-transfer coefficient boundary conditions of the dropwise condensation problem lead to constriction conductances proportional to a power of the surface thermal conductivity slightly less than 1.0. As the applied coefficients increase in absolute magnitude, however, the situation becomes more and more like the applied heat flux step function boundary condition. As the Nusselt number $\bar{h}_d \hat{r}/k_l$ increases, one would thus expect m to decrease, and this behavior is observed.

Figure 7 displays curves for C and m as functions of the pertinent dimensionless variables, obtained by a least-squares fit to equation (16) of numerous data generated via a computer-coded, many-drop-class version of the algorithm of Section 4. The range of independent variables shown should suffice for most dropwise condensation situations of interest.

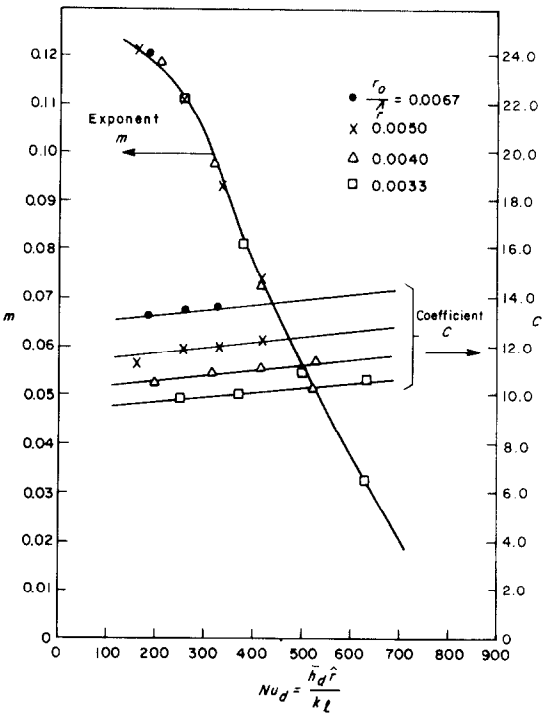

FIG. 7. Constants for use in the constriction resistance correlation.

The coefficient C is found to vary only by about 27% over the range of parameters considered, and the exponent m also does not change radically. Sensitivity of the results to parameters which are somewhat uncertain is not overly great; for example, a 25% increase in the departing drop size $\hat{r}$ yields about the same fractional increase in the constriction resistance. Note that for purposes of the correlation, a cutoff radius $r_0 = 0.0005$ cm is appropriate.

For steam at atmospheric pressure, with negligible noncondensable gas concentrations, appropriate values for the asymptotic surface conductance $\bar{h}_d$ and departing drop size $\hat{r}$ are 2.27×10^5 W/m^2 K and 0.125 cm, respectively. These values lead to the result

$$Bi_c = 11.24\left(\frac{k}{k_l}\right)^{-0.074} \tag{18}$$

for the constriction conductance.

The thermal constriction resistance calculated from equation (18) is to be added in series with the distribution-averaged droplet resistance. The overall steamside Biot number can then be written as

$$Bi = Bi_d\left[1 + Bi_d \Big/ \left(11.24\left(\frac{k}{k_l}\right)^{-0.074}\right)\right]^{-1} \tag{19}$$

in which

$$Bi = \frac{h\hat{r}}{k}, \tag{20}$$

and

$$Bi_d = \frac{\bar{h}_d \hat{r}}{k}. \tag{21}$$

The relationships (18) and (19) are applicable to atmospheric pressure steam condensation on vertical, relatively smooth surfaces, with minimal noncondensable gas concentration. For the important case of subatmospheric pressure condensation, a relationship derived from the experiments of Graham [17] can be used for the asymptotic conductance together with Fig. 7 in order to estimate the constriction resistance:

$$\bar{h}_d = 1.98 \times 10^3 T_{sat} + 0.29 \times 10^5 \qquad (22)$$

in which the asymptotic conductance $\bar{h}_d$ is expressed in $W/m^2 K$ and the saturation temperature T_{sat} is in °C.

Small concentrations of noncondensable gases, rough surfaces, and condenser orientations far from the vertical can be accounted for through the use of suitable choices of $\bar{h}_d$ and $\hat{r}$.

The analysis described here is also appropriate for fluids other than water, provided that the resultant contact angles are close to 90° (contact angles far from 90° may lead to altered macroscopic drop distributions).

The crucial test for any model is comparison to experimental data. Equation (19) was used to generate the solid curve in Fig. 8, which also contains the results of the studies mentioned in Section 2 (except for those of [12] relating to a horizontal surface).

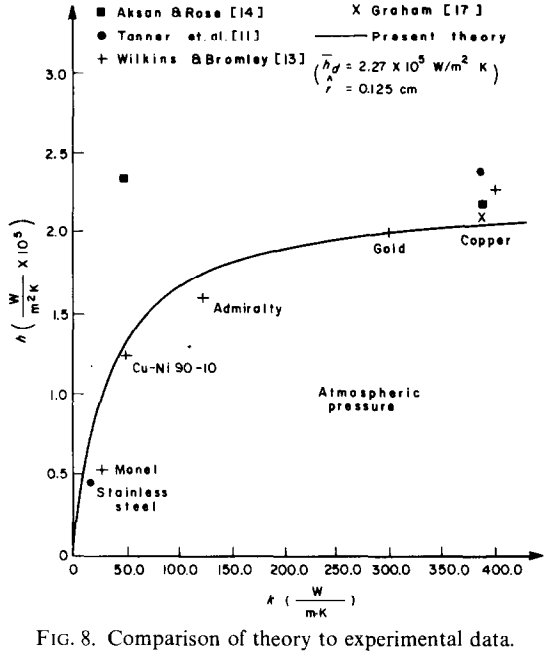

FIG. 8. Comparison of theory to experimental data.

The agreement is seen to be excellent with the exception of a single anomolous data point. Although space does not allow for a detailed discussion of the experimental data, it should be noted that this anomalous point was obtained using the standard extrapolation method of surface temperature measurement, which is highly inaccurate for low conductivity materials.

Since some differences in the asymptotic conductance $\bar{h}_d$ and departure size $\hat{r}$ from experiment to experiment are to be expected, as well as the numerous sources of experimental error, the slight differences between the theory and the majority of data points is not surprising.

6. CONCLUSION

Due to the finite lateral thermal conductivity of the condensing surface material, the distribution of droplets of varying size over the surface during dropwise condensation and the resulting inhomogeneity of surface heat flux induces a thermal resistance in addition to the average droplet resistance. This resistance, the thermal constriction resistance, was studied analytically and the results compared to available data in the work described herein.

The analytical model, consisting of a synthesis of single-drop constriction resistance results with known droplet distribution information, resulted in a correlation for the overall dropwise condensation constriction conductance as a function of the condensing surface thermal conductivity.

The correlation is simple in form and agrees well with the bulk of available experimental evidence.

Acknowledgements—This work was supported by Bell Telephone Laboratories and the National Science Foundation.

REFERENCES

1. E. Schmidt, W. Schurig and W. Selschopp, Versuche uber die kondensation von wasserdampf in film-und tropenform, *Tech. Mech. Thermo-Dynam., Berl.* **1**, 53 (1930).
2. M. Jakob, Heat transfer in evaporation and condensation—II, *Mech. Engng* **58**, 729 (1936).
3. E. LeFevre and J. Rose, A theory of heat transfer by dropwise condensation, in *Proceedings of the 3rd International Heat Transfer Conference*, Part II, p. 362. A.I.Ch.E., New York (1966).
4. C. Graham and P. Griffith, Drop size distributions and heat transfer in dropwise condensation, *Int. J. Heat Mass Transfer* **16**, 337–346 (1973).
5. E. Gose, A. Mucciardi and E. Baer, Model for dropwise condensation on randomly distributed sites, *Int. J. Heat Mass Transfer* **10**, 15–22 (1967).
6. I. Tanasawa and F. Tachibana, A synthesis of the total process of dropwise condensation using the method of computer simulation, in *Proceedings of the 4th International Heat Transfer Conference*, Part VI, paper Cs 1.3. A.I.Ch.E., New York (1970).
7. I. Tanasawa, F. Tachibana and J. Ochia, A study of the process of drop growth by coalescence during dropwise condensation, *Bull. J.S.M.E.* **16**(99), 1367 (1973).
8. L. Glicksman and A. Hunt, Numerical simulation of dropwise condensation, *Int. J. Heat Mass Transfer* **15**, 2251–2269 (1972).
9. B. Mikic, On mechanism of dropwise condensation, *Int. J. Heat Mass Transfer* **12**, 1311–1323 (1969).
10. J. Rose and L. Glicksman, Dropwise condensation—the distribution of drop sizes, *Int. J. Heat Mass Transfer* **16**, 411–425 (1973).
11. D. Tanner, D. Pope, C. Potter and D. West, Heat transfer in dropwise condensation—Part II, *Int. J. Heat Mass Transfer* **8**, 427–436 (1965).
12. P. Griffith and M. Lee, The effect of surface thermal properties and finish on dropwise condensation, *Int. J. Heat Mass Transfer* **10**, 697–707 (1967).
13. D. Wilkins and L. Bromley, Dropwise condensation phenomena, *A.I.Ch.E. Jl* **19**, 839 (1973).
14. S. Aksan and J. Rose, Dropwise condensation—the effect of thermal properties of the condenser material, *Int. J. Heat Mass Transfer* **16**, 461–467 (1973).

15. M. G. Cooper, B. B. Mikic and M. M. Yovanovich, Thermal contact conductance, *Int. J. Heat Mass Transfer* **12**, 279-300 (1969).
16. R. Hannemann, An examination of dropwise condensation phenomena, including the effect of surface thermal conductivity on the rate of heat transfer, Sc.D. Thesis, Massachusetts Institute of Technology (1975).
17. C. Graham, The limiting heat transfer mechanism of dropwise condensation, Ph.D. Thesis, Massachusetts Institute of Technology (1969).
18. I. Tanasawa and J. Ochiai, Experimental study of the dropwise condensation process, *Trans. J.S.M.E.* **38**(316), 3193 (1972).

APPENDIX

The fundamental single-drop constriction resistance problem is illustrated in general terms in Fig. 9. A radial step function variation in heat-transfer coefficient is imposed on a cylinder of radius R of material of conductivity k; the top surface is exposed to vapor at temperature T_v. The cylinder length is L and the surface $r = R$ is assumed insulated. The surface at $z = L$ is taken to be at constant temperature T_0.

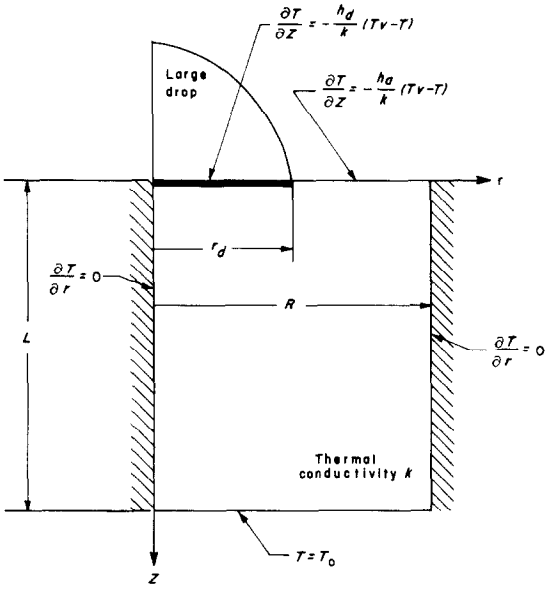

FIG. 9. The fundamental single-drop constriction resistance problem.

Defining the dimensionless variables

$$\left.\begin{aligned} \rho &= \frac{r}{R}, \quad \zeta = \frac{z}{R}, \quad \eta = \frac{r_d}{R} \\ \gamma &= \frac{h_d}{h_a}, \quad \theta = \frac{T - T_0}{T_v - T_0}, \\ Bi_d^* &= \frac{h_d R}{K}, \quad Bi_a = \frac{h_a R}{k}, \end{aligned}\right\} \tag{A.1}$$

the equation to be solved becomes

$$\frac{1}{\rho}\frac{\partial}{\partial \rho}\left(\rho \frac{\partial \theta}{\partial \rho}\right) + \frac{\partial^2 \theta}{\partial \zeta^2} = 0 \tag{A.2}$$

with the transformed boundary conditions

$$\left.\begin{aligned} &\theta\left(1, \frac{L}{R}\right) = 0 \\ &\left.\frac{\partial \theta}{\partial \rho}\right|_{\rho=0} = \left.\frac{\partial \theta}{\partial \rho}\right|_{\rho=1} = 0 \\ &\left.\frac{\partial \theta}{\partial \zeta}\right|_{\zeta=0} = Bi_d^*(\theta - 1), \quad 0 < \rho \leqslant \eta \\ &\left.\frac{\partial \theta}{\partial \zeta}\right|_{\zeta=0} = Bi_a(\theta - 1), \quad \eta < \rho < 1 \end{aligned}\right\} \tag{A.3}$$

A closed form analytical solution for this problem is apparently not obtainable. For use in the dropwise condensation constriction resistance model, a finite element computer program was employed for a solution over a wide range of dimensionless parameters. It was found that a dimensionless cylinder height $L/R = 4$ gave a uniform temperature profile near the bottom of the cylinder and so produced the full constriction effect.

In the results shown in Fig. 4, the temperature data obtained was used to calculate the thermal constriction conductance and this information was catalogued in a form useful in the later modeling. In that figure, $Bi_s = h_s R/k$ is the dimensionless, area-averaged preconstriction heat-transfer coefficient while $Bi_c^* = h_c R/k$ is the dimensionless constriction conductance.

ETUDE ANALYTIQUE DE L'INFLUENCE DE LA CONDUCTIVITE THERMIQUE DE PAROI SUR LE TRANSFERT DE CHALEUR PAR CONDENSATION EN GOUTTES

Résumé—On présente une étude analytique de l'influence des propriétés thermiques du matériau constituant le condenseur sur le coefficient de transfert de chaleur par condensation en gouttes. Les solutions obtenues de résistance due à la striction pour une goutte isolée sont associées à une distribution connue des gouttes et conduisent à une relation simple qui décrit l'effet étudié. La relation obtenue est en bon accord avec la plupart des données expérimentales connues pour l'eau; d'autres fluides peuvent être traités suivant le schéma analytique développé.

EINE ANALYSE DES EFFEKTS DER WÄRMELEITFÄHIGKEIT DES KÜHLKÖRPERS AUF DEN WÄRMEÜBERGANG BEI TROPFENKONDENSATION

Zusammenfassung—Es wird über eine Analyse des Einflusses der thermischen Eigenschaften des Kühlkörpermaterials auf den Wärmeübergangskoeffizienten bei Tropfenkondensation berichtet. Die Synthese von Lösungen für den Einschnürungswiderstand von Einzeltropfen führt bei bekannter Tropfenverteilung zu einer einfachen Beziehung. Diese Beziehung stimmt gut überein mit der Mehrzahl der bekannten Versuchsergebnisse für Wasser; andere Fluide können auf dem angegebenen analytischen Weg behandelt werden.

ВЛИЯНИЕ КОЭФФИЦИЕНТА ТЕПЛОПРОВОДНОСТИ МАТЕРИАЛА ПОВЕРХНОСТИ НА ИНТЕНСИВНОСТЬ ТЕПЛООБМЕНА ПРИ КАПЕЛЬНОЙ КОНДЕНСАЦИИ

Аннотация — В статье анализируется влияние теплофизических свойств материала конденсатора на коэффициент теплообмена при капельной конденсации. Простое соотношение для данного эффекта получено на основе синтеза решений для сопротивления сжатию отдельной капли с помощью известного распределения капель. Данное соотношение хорошо согласуется с имеющимися экспериментальными данными для воды; другие жидкости могут быть рассмотрены уже разработанным аналитическим способом.